Published in final edited form as:
Dev Biol. 2012 October 15; 370(2): 165–172. doi:10.1016/j.ydbio.2012.07.020.

The role of Bicoid cooperative binding in the patterning of sharp borders in *Drosophila melanogaster*

F.J.P. Lopes[*,1], **A.V. Spirov**[2,3], and **P.M. Bisch**[1]

[1]Instituto de Biofisica Carlos Chagas Filho, Universidade Federal do Rio de Janeiro, Rio de Janeiro, RJ, 21941-902, Brazil.

[2]Laboratory of Evolutionary Modelling, the Sechenov Institute of Evolutionary Physiology and Biochemistry of the Russian Academy of Sciences, Saint-Petersburg, Russia.

[3]Computer Science Department and Center of Excellence in Wireless & Information Technology, State University of New York at Stony Brook, 500 Stony Brook Road, Stony Brook, NY, USA.

Abstract

In *Drosophila* embryonic development, the Bicoid (Bcd) protein establishes positional information of downstream developmental genes like *hunchback* (*hb*), which has a strong anterior expression and a sharp on-off boundary in the mid-embryo. The role of Bcd cooperative binding in the positioning of the Hb pattern has been previously demonstrated. However, there are discrepancies in the reported results about the role of this mechanism in the sharp Hb border. Here, we determined the Hill coefficient (n_H) required for Bcd to generate the sharp border of Hb in wild-type (WT) embryos. We found that an n_H of approximately 6.3 (*s.d.* 1.4) and 10.8 (*s.d.* 4.0) is required to account for Hb sharpness at early and late cycle 14A, respectively. Additional mechanisms are possibly required because the high n_H is likely unachievable for Bcd binding to the *hb* promoter. To test this idea, we determined the n_H required to pattern the Hb profile of 15 embryos expressing an hb^{14F} allele that is defective in self-activation and found n_H to be 3.0 (*s.d.* 1.0). This result indicates that in WT embryos, the *hb* self-activation is important for Hb sharpness. Corroborating our results, we also found a progressive increase in the required value of n_H spanning from 4.0 to 9.2 by determining this coefficient from averaged profiles of eight temporal classes at cycle 14A (T1 to T8). Our results indicate that there is a transition in the mechanisms responsible for the sharp Hb border during cycle 14A: in early stages of this cycle, Bcd cooperative binding is primarily responsible for Hb sharpness; in late cycle 14A, *hb* self-activation becomes the dominant mechanism.

Keywords

Drosophila melanogaster; Bicoid; *hunchback*; cooperative binding; Hill coefficient; self-regulation

[*]corresponding author:Phone: +55 21 2562 6571; FAX +55 21 2280 8193 flopes@ufrj.br.

ACCESSION NUMBERS Bicoid (Gene ID: 40830) Hunchback (ID: 41032)

INTRODUCTION

It has been shown that cooperative binding plays a central role in pattern formation and in the interpretation of morphogenetic positional information during embryonic development. One classical example is the Bicoid (Bcd) protein that establishes the anterior–posterior (AP) developmental axis during embryonic development in *Drosophila melanogaster*. This morphogenetic protein determines positional information for downstream developmental genes such as *hunchback* (*hb*), *Krüppel* (*Kr*) and *knirps* (*kni*), which also show cross-regulation (Berleth et al., 1988; Crauk and Dostatni, 2005; de Lachapelle and Bergmann, 2010; Driever and Nusslein-Volhard, 1988; He et al., 2010a; Jäckle et al., 1986; Jaeger et al., 2004; Manu et al., 2009; Nusslein-Volhard et al., 1987; Papatsenko and Levine, 2011). It has been shown that cooperative binding is critical for Bcd transcriptional activity (Burz and Hanes, 2001; Burz et al., 1998; Driever et al., 1989; Lebrecht et al., 2005; Lopes et al., 2005; Lopes et al., 2008; Ma et al., 1996) and plays a central role in reducing transcriptional noise during Drosophila development (Holloway et al., 2011).

The *hb* gene encodes a morphogenetic protein (Lehmann and Nusslein-Volhard, 1987; Papatsenko and Levine, 2008; Tautz et al., 1987) and exhibits anterior and posterior expression patterns (Fig. 1). The *hb* regulatory region has two distinct promoters, P1 (distal) and P2 (proximal); each controls the expression of specific transcripts that encode the same protein (Margolis et al., 1995; Spirov et al., 2002; Spirov et al., 2000; Tautz et al., 1987)[1]. In the anterior region of the embryo, the regulation of *hb* by Bcd and Hb proteins (Driever and Nusslein-Volhard, 1989; Lukowitz et al., 1994; Margolis et al., 1995; Simpson-Brose et al., 1994; Struhl et al., 1989; Treisman and Desplan, 1989) produces a uniform expression pattern with a sharp on–off boundary at mid-embryo (Fig. 1). It was shown that an ~300 bp region upstream of the *hb* coding region, the core part of the proximal promoter, that contains 6 main Bcd sites is sufficient to confer full regulation of *hb* by Bcd (Driever et al., 1989; Schroder et al., 1988; Struhl et al., 1989). Cooperative binding of Bcd to these six sites has also been previously demonstrated (Burz et al., 1998; Lopes et al., 2005; Ma et al., 1996). Moreover, to show that Bcd cooperative binding could determine the positioning of the *hb* pattern, Driever et al. used a series of lacZ artificial constructs that were driven by fragments of the native *hb* promoter and contained different numbers of Bcd binding sites (Driever et al., 1989). It was then suggested that this mechanism could account for the sharpness of the *hb* pattern because the sharpness of the lacZ patterns increased with the number and strength of Bcd sites. However, none of the lacZ constructs analyzed achieved wild-type (WT) Hb sharpness. This result was found even when an artificial construct was driven by 6 strong and 6 weak Bcd sites, which showed the strongest level of expression. Since these experiments, many efforts have been dedicated to characterizing the role of Bcd cooperative binding in *hb* pattern formation (Burz et al., 1998; Crauk and Dostatni, 2005; Gregor et al., 2007a; Lebrecht et al., 2005; Lopes et al., 2005; Lopes et al., 2008; Ma et al., 1996).

He et al. contributed to the above discussion with immunofluorescence to determine Bcd and Hb protein profiles from 28 WT embryos at early cycle 14A and found that a Hill coefficient (n_H) of approximately 5.1 ± 2.7 in the dorsal and 4.9 ± 2.7 in the ventral side was sufficient to account for Hb sharpness (He et al., 2010b). Using the same technique with 9 early embryos at cycle 14A and visual inspection, Gregor et al. found an n_H of approximately 5.0 (Gregor et al., 2007a). This result indicates that Bcd cooperative binding is sufficient to account for *hb* regulation. However, the coefficients required are higher than those that are observed experimentally. Using DNAse footprint assays *in vitro*, an estimated n_H of 3.6 was found for Bcd binding to a 250 bp fragment of the native *hb* promoter

[1]For details http://www.evol.nw.ru/spirov/hox_pro/hunchback.html

containing the six Bcd strong sites (Ma et al., 1996). Using gel-shift assays, the n_H was estimated as 3.0 (*standard deviation*, *s.d.* 0.031) for the binding of a homeodomain-containing fragment of Bcd (called Bcd89–154) to a 230 bp *hb* element also containing the six Bcd strong sites (Burz et al., 1998). Using immunofluorescence and fluorescent *in situ* hybridization (FISH), early embryos at cycle 14A (He et al., 2011) were used to show that the n_H required for Bcd to pattern the *hb* transcriptional profile (6.1±2.6, calculated from 14 embryos) was higher than the coefficient required to pattern the Hb protein profile (5.2±0.4, calculated from 5 embryos). In addition, Houchmandzadeh et al. have suggested that Bcd alone cannot account for Hb sharpness because an n_H of more than 10 is required based on their estimations (Houchmandzadeh et al., 2002). Finally, the idea that Hb sharpness is caused by *hb* self-activation through bistable kinetics was proposed based on work using a systems biology approach that combined immunofluorescence and a reaction-network model (Lopes et al., 2008).

During cycle 14A, the *hb* expression pattern exhibits a significant variation of approximately 30% (Lopes et al., 2008; Surkova et al., 2008) and reaches a maximum level of expression around mid-cycle. Bcd protein concentration, in turn, decreases continuously from its maximum level at the beginning of the cycle (Gregor et al., 2007b; Surkova et al., 2008). These patterns of temporal variation indicate that the contribution of both Bcd and Hb proteins must be temporally modulated and that a precise characterization of Bcd cooperative binding and *hb* self-activation in Hb sharpness must account for the variations in different stages of cycle 14A.

Here, we analyzed Bcd cooperativity levels using 30 WT Bcd and Hb profiles. We found that an n_H of 6.3 (*s.d.* 1.4) is required to account for Hb sharpness at early cycle 14A. However, at late stages of this cycle, an n_H of approximately 10.8 (*s.d.* 4.0) is required. Bcd binding is not likely to reach this level of cooperativity. Thus, we investigated additional regulation that could be taking place by determining the n_H required to pattern the Hb profile of 15 embryos expressing an hb^{14F} allele that is defective in self-regulation. We found an n_H of 3.0 (*s.d.* 1.0), which is in agreement with previous *in vitro* results (Burz et al., 1998; Ma et al., 1996). This result indicates that *hb* self-activation contributes to Hb sharpness in WT embryos, which was suggested in earlier studies (Lopes et al., 2008; Simpson-Brose et al., 1994). We verified our results using an independent set of data (Poustelnikova et al., 2004; Surkova et al., 2008) to follow the progressive increase in the n_H required to account for Hb sharpness from early to late cycle 14. Taken together, our results indicate that there is a transition in the mechanisms responsible for *hb* sharpness during cycle 14A: in early stages of this cycle, Bcd cooperative binding is mainly responsible for *hb* sharpness; in late cycle 14A, *hb* self-activation becomes the dominant mechanism.

MATERIALS AND METHODS

Dataset

WT Oregon-R and *hb* mutant hb^{14F} (Hülskamp et al., 1994) embryos were stained for Bcd and Hb proteins. For the pThb5 construct (driven by a fragment of the *hb* promoter (Driever et al., 1989)), lacZ expression was visualized by FISH. These data were previously used in different analysis (Holloway et al., 2011; Lopes et al., 2008).

Embryo fixation and staining

Embryos were incubated with guinea pig and rat primary antibodies against Hb and Bcd, respectively, followed by secondary antibodies labeled with Alexa Fluor 647 (to Hb) and 488 (to Bcd; Molecular Probes). For lacZ embryos, simultaneous immunostaining was used to detect Hb and Bcd, and FISH was used to detect lacZ transcripts using the Janssens et al.

method (Janssens et al., 2005). Immunostaining was performed as above to detect Hb (Alexa Fluor 647) and Bcd (Alexa Fluor 555). After hybridization, lacZ mRNA was visualized by sequential incubation with a rabbit antibody to fluorescein (Molecular Probes) and then an antibody to rabbit labeled with Alexa Fluor 488 (Molecular Probes).

Confocal Microscopy

Whole-embryo images were taken using a laser confocal scanning microscope (Leica TCS SP2) and the Janssens et al. method (Janssens et al., 2005). Fluorophores were excited by a laser at different wavelengths (488, 555, and 647 nm) and detected via a filterless spectral separation system. To reduce image noise from the photomultiplier tubes, each embryo was scanned sequentially 16 times, and the results were averaged.

Image Processing

Protein and RNA profiles were determined by averaging intensities in each dorsoventral pixel column from the central 10% strip of the AP axis. The quality of this direct method was checked by nuclear masks that were manually made based on several costained lacZ embryos using the multiple ROI feature in ImageJ software (Moodley and Murrell, 2004). Each circular ROI with radii comparable to the nuclear radii was manually positioned to outline a given nucleus. Nuclear-resolution AP profiles from this method were of comparable quality to pixel-resolution profiles from our direct extraction method.

Temporal Classification

In addition to confocal scanning, all embryos were observed along the dorsal edge using Differential Interference Contrast (DIC) optics. Distances were measured from the egg surface to the invaginating membrane and from the surface to the cortex. The ratio of the membrane depth to the cortex depth was used to estimate the embryo age in minutes using a published standard curve (Merrill et al., 1988).

The straight line fitting of the Hill equation

The original form of the Hill equation can be written as (Hill, 1910):

$$Fr=\frac{[L]^{n\mathrm{H}}}{K+[L]^{n\mathrm{H}}} \tag{1}$$

In this equation, used to generate the plots of Fig. 3, Fr is the fraction of site occupancy, i.e. the number of bound sites by the total number of sites, n_{H} is the Hill coefficient, $[L]$ is the (total) ligand concentration and K the equilibrium constant. This constant is related to $[L]_{1/2}$, the ligand concentration that produces half of promoter occupancy, by $K=[L]_{1/2}^{n_{\mathrm{H}}}$.

For practical applications, it is useful to write the above equation as

$$\ln\left(\frac{Fr}{1-Fr}\right)=n_{\mathrm{H}}\ln\left(\frac{[L]}{[L]_{1/2}}\right) \tag{2}$$

This equation can be easily used in a linear fitting to determine n_{H}, which is the inclination of the straight line. This procedure was used to generate the plots of Figs. 2 and 4.

A recent result has shown that the protein signal obtained from immunostaining experiments is proportional to the real protein concentration (Gregor et al., 2007a). Using this result, we determined $[L]/[L]_{1/2}$ as the quotient $[\mathrm{Bcd}_{\mathrm{signal}}]/[\mathrm{Bcd}_{\mathrm{signal}}]_{1/2}$. In this relation, $[\mathrm{Bcd}_{\mathrm{signal}}]$ is the signal intensity of the Bcd protein at each position in the AP axis of the Drosophila

embryo and $[Bcd_{signal}]_{1/2}$ is the $[Bcd_{signal}]$ observed at the position where half of the Hb protein signal is detected. To determine *Fr* we assume that the level of protein signal is proportional to the fraction of site occupancy (Gregor et al., 2007a; He et al., 2010b). This assumption allowed us to determine *Fr* as the quotient $[Hb_{signal}]/[Hb_{signal}]_{max}$. In this relation, $[Hb_{signal}]$ is the signal intensity of the Hb protein at each position in the AP axis and $[Hb_{signal}]_{max}$ is the maximum level of Hb protein signal. To fit the equations (1) and (2), a region of interest (ROI) in the posterior border of the anterior Hb pattern was defined. We used a ROI in the range of 5% to 95% of the maximum Hb profile. This ROI was based on Gregor et al results about the 10% accuracy for the detection of protein concentrations (Gregor et al., 2007a). In addition, this ROI accounts for the estimated error level introduced by confocal images (Myasnikova et al., 2009).

Fitting procedures

Fitting was performed using the Matlab platform with the respective equations for *root mean square deviation* (*r.m.s.d.*) and *standard deviation* (*s.d.*):

$$rmsd=\sqrt{\frac{1}{m}\sum_{i=1}^{m}(exp_i - the_i)^2} \quad (3)$$

and

$$sd=\sqrt{\frac{1}{m}\sum_{i=1}^{m}(exp_i - \mu)^2} \quad (4)$$

where "*exp*" is the experimental data and "*the*" is the corresponding theoretical values for each position *i* along the AP axis in the embryo. *m* and μ are the number of experimental points and its mean, respectively.

RESULTS

Bcd cooperative binding cannot account for late Hb sharpness

Here we are not estimating n_H or analyzing the *bcd/hb* relationship. In our analysis, we are estimating the Hill coefficient required for generating the sharpness of the *hb* expression pattern in WT and hb^{14} mutant embryos. In order to analyze the ability of the Bcd gradient to generate each *hb* pattern, we compared this estimated n_H with the experimentally determined values.

To determine what value of n_H is necessary for Bcd cooperative binding to produce the sharp Hb border, we used 15 embryos at early cycle 14A and found an n_H of 6.3 (*s.d.*, 1.4, Fig. 2A; Table 1). This is in agreement with similar results for early embryos found by He et al. (He et al., 2011; He et al., 2010b) and Gregor et al. (Gregor et al., 2007a). To test what n_H is necessary to account for mature Hb sharpness, we used 15 embryos at late cycle 14A and found an n_H of 10.8 (*s.d.* 4.0, Fig. 2B; Table 1). This coefficient value is approximately three times that of the coefficient estimated for human hemoglobin (n_H = 2.8 (Stryer, 1995)) and is not likely to ever be reached by Bcd binding to the six sites shown to be sufficient to reproduce *hb* regulation by Bcd (Driever et al., 1989; Schroder et al., 1988; Struhl et al., 1989).

Gregor et al. based their results on early embryos at cycle 14 to reduce the influence of other transcriptional regulators on Hb profiles as much as possible (Gregor et al., 2007a). The authors found that n_H = 5.0 and suggested that Bcd cooperative binding accounts for *hb*

regulation in early embryos. To verify the effect of embryo age using the Gregor et al. approach, we plotted our Bcd/Hb data from early and late embryos in the same semi-log plot that they used. We found that the ratios between the axis for early (Fig. 3A, very similar to Fig. 4A in Gregor et al. (Gregor et al., 2007a)) and late embryos (Fig. 3B) are different and result in different coefficient estimations: 6 for early and 10 for late embryos. Although similar values were found using both of the above approaches, the latter is less appropriate because a visual inspection was used and the differences between the plots for early and late embryos were not as evident as for the straight lines (Fig. 2A,B).

These results indicate that Bcd plays a critical role in sharpening early Hb profiles but cannot fully account for the sharpness of the mature Hb pattern; thus, other regulators must be performing a role in sharpening the Hb pattern. Below, we estimated n_H values for Bcd binding to the endogenous *hb* regulatory region in WT embryos and tested the role of additional regulators.

hb self-activation is critical for Hb sharpness

The role of *hb* self-activation in the sharpness of the Hb pattern has previously been demonstrated (Lopes et al., 2008). This effect is more evident in late embryos due to Hb protein accumulation. Therefore, to perform a confident estimation for the effect of additional regulation, it is necessary to determine *hb* self-regulatory effects.

Performing this estimation is possible using hb^{14F} embryos, which harbor an *hb* allele that is deficient for self-activation (Hülskamp et al., 1994; Lopes et al., 2008). Using 15 embryos, we found that an n_H of approximately 3.0 (*s.d.* 1.0, Fig. 2C) is required to account for Hb pattern in this allele. This coefficient value is in good agreement with the 3.6 and 3.0 (*s.d.* 0.031) found by Ma et al. and Burz et al. (Burz et al., 1998), respectively. However, these values are significantly lower than our estimations for the n_H required to pattern the Hb profile at early (6.3 *s.d.* 1.4) or late (10.8 *s.d.* 4.0) cycle 14A. This difference suggests that in WT embryos the n_H value required to pattern the Hb profile is affected by other mechanisms, most likely *hb* self-activation.

To check the effect of additional regulation on Hill coefficients, we used the patterns of beta-galactosidase transcripts from 9 early embryos expressing a lacZ construct driven by a fragment of the native *hb* promoter (pThb5 (Driever et al., 1989)) that contained six Bcd, two Hb and two Kr sites (Treisman and Desplan, 1989) (Fig. 2D). We reasoned that visualizing lacZ transcripts instead of β-galactosidase protein would give results that are more accurate because transcripts can be degraded normally, as other endogenous transcripts are. Using this visualization approach, we found that an n_H of 7.0 (*s.d.* 1.5) is required to pattern the profile of the lacZ transcripts. This n_H value is higher than the n_H estimated to pattern the Hb profile in early (6.3, *s.d.* 1.4) cycle 14A embryos but lower than the estimation for late (10.8, *s.d.* 4.0) cycle 14A embryos. Our result quantitatively shows that additional regulation of the target gene can affect the determination of the Hill coefficient.

The cooperative-binding and self-regulating stages of Hb pattern formation

To verify the above results using an independent set of experimental data, we used quantitative data from the FlyEx (Poustelnikova et al., 2004; Surkova et al., 2008) database (http://urchin.spbcas.ru/flyex or http://flyex.uchicago.edu/flyex/index.jsp), which divides cycle 14A into 8 time classes, T1 to T8. We used the averaged (integrated) data for Bcd and Hb protein profiles, which are very close to the profiles of individual embryos. This approach allowed us to estimate the required Hill coefficient necessary for Bcd to produce the Hb pattern at each temporal class (Fig. 4). We found that the required n_H varies from 4.0 (*r.m.s.d.*, 0.13; at T1) to 9.2 (*r.m.s.d.* 0.41; at T7; Fig. 4I) (see Materials and Methods for

definition of *r.m.s.d.*). The required n_H at T1 (4.0, *r.m.s.d.* 0.13) is also in agreement with our estimation using hb^{14F} (3.0, *s.d.* 1.0), the estimation of Burz et al. (Burz et al., 1998) (3.0, *s.d.* 0.031) and the estimation of Ma et al. (Ma et al., 1996) (3.6). These data also indicate that the *bcd*/hb^{14F} pair and the WT *bcd*/*hb* (at T1) are the only cases where Hb sharpness is fully produced by Bcd cooperative binding. Moreover, even though Bcd cooperative binding is performing a critical role for Hb sharpness during time classes T2 (n_H 4.6, *r.m.s.d.* 0.16) and T3 (n_H = 5.2, *r.m.s.d.* 0.15), it cannot account for the overall sharpness of Hb expression. Furthermore, the required n_H ranges from 6.0 to 9.2 for the T5 to T8 stages (Fig. 4I) and makes it even less feasible that Bcd cooperativity alone accounts for the Hb sharpness. Even in the T4 stage, where the required n_H is 6.0, Bcd could not solely account for the Hb sharpness because only three of the six main Bcd binding sites are strong (Driever and Nusslein-Volhard, 1989); thus, the maximum n_H of 6 is not feasible. The effect of *hb* self-activation is more pronounced after Hb protein accumulation because *hb* self-activation plays a critical role in Hb sharpness (Lopes et al., 2008). The above results suggest that cycle 14A occurs in two distinct stages: a stage that relies predominantly on Bcd cooperative binding from T1 until T4 (the first 24 minutes of the cycle) and a stage that relies predominantly on self-regulation by Hb from T4 until T8 (the remaining 24 minutes).

The early stages of the *bcd/hb* system are best described by the Hill approach

To check the applicability of the Hill approach to the *bcd/hb* system, we determined the *r.m.s.d.* for the coefficient fitting of each time class in the averaged data (Fig. 4I). We observed a five-fold increase in the *r.m.s.d.* from 0.13 for T1 to 0.69 for T8. This increase indicates that T1 is the best time class for the application of the Hill approach. This finding is expected because the n_H of 4.0 for T1 is similar to the n_H found for hb^{14F}, the self-activation mutant where the *hb* pattern exhibits only the effect of Bcd cooperative binding. The progressive increase in *r.m.s.d.* after T1 (*r.m.s.d.* in T4, 0.30, is more than two times higher than that of T1, 0.13) also indicates that the *bcd/hb* system is progressively less accurately described by this approach. This loss of appropriateness results from the progressive accumulation of Hb protein, which shows a maximum concentration at mid-cycle 14A (Lopes et al., 2008; Surkova et al., 2008). The observed increase in *r.m.s.d.* is in agreement with the division of cycle 14A into cooperative (T1 until T4) and self-regulating (T4 until T8) stages.

To perform a similar analysis of Hill equation fitting for the unaveraged data shown in Fig. 2, it was unsuitable to use *r.m.s.d.* because this measurement would be indistinguishable from the effects of intrinsic transcriptional noise (He et al., 2010a; Holloway et al., 2011) and from fitting by the Hill approach. To circumvent this limitation, we used the *standard deviation* (*s.d.*) because we used 15 embryos for each assay except for the 9 embryos used for the pThb5 lacZ construct. From the mean *s.d.* for hb^{14F} (1.02), early WT (1.45), late WT (6.08) and the lacZ construct (1.52), we note that the *bcd*/hb^{14F} system is the one better described by the Hill approach, as describe above. The early WT, lacZ, and late WT embryos each show a progressive increase in the mean *s.d.*, which indicates that these systems are progressively more poorly described by the Hill approach. This result is consistent with the increased effect of *hb* self-activation in these systems. Taken together, these results indicate that the *r.m.s.d.* and *s.d.* of the straight-line fitting of the Hill equation can be used to verify the applicability of the Hill approach.

DISCUSSION

Driever et al. first suggested that Bcd cooperative binding could account for Hb sharpness (Driever et al., 1989). Since then, there have been studies that demonstrate that Bcd cooperative DNA binding occurs; however, discrepant results exist about whether the resulting effects are sufficient to account for the sharp borders of expression observed for

Hb and other Bcd target genes. In particular, the importance of Hb self-activation has been the subject of debate. To help resolve these discrepancies, we estimated the n_H required to pattern Hb profile in the hb^{14F} self-activation mutant allele, which does not exhibit *hb* self-regulation. Analysis of this mutant allowed us to distinguish contributions to the overall n_H by both Bcd cooperativity and by Hb self-activation. The n_H of 3.0 (*s.d.* 1.0) that we found from hb^{14F} embryos agrees with the n_H values for Bcd binding to fragments of the *hb* promoter containing the six main Bcd binding sites of 3.6 and 3.0 (*s.d.* 0.031) from Ma et al. (Ma et al., 1996) and Burz et al. (Burz et al., 1998), respectively. Although these values seem contradictory to others in the literature (Gregor et al., 2007a; He et al., 2011; He et al., 2010b), we detail below how these values are in fact explainable.

A time resolved analysis was needed to understand the role of Bcd cooperative binding in *hb* patterning because Bcd and Hb patterns show significant variation during cycle 14A. By performing this analysis, we found that Bcd cooperative binding does account for Hb sharpness at very early stages of cycle 14A because the required n_H for time class T1 is similar to that estimated for hb^{14F} (Fig. 4I, Table 1). This result indicates that Hb protein (from zygotic or embryonic origin) must have little or no role in the sharpness of very early Hb patterning. For time classes T2 to T4, however, the effect of *hb* self-activation increases because the required n_H increases progressively (Fig. 4I). This increase in n_H agrees with the n_H we found for cycle 14A (Table 1). Taken together with the progressive decrease in Bcd and increase in Hb concentrations (Gregor et al., 2007b; Surkova et al., 2008), these results indicate that a combination of well-established Bcd cooperative binding and nascent self-regulatory effects are important for the establishment of Hb sharpness for time classes T1 until T4. Self-regulation becomes predominant as reflected in the n_H for time classes T5 to T8 and in late WT embryos (Fig. 4I, Table 1). This driven change is in agreement with the ability of Bcd cooperative binding to determine the positioning of the *hb* pattern (Driever et al., 1989; Lopes et al., 2008) because positioning is determined in the early stages of cycle 14 (Fig. 2C in Lopes et al. (Lopes et al., 2008) and Fig. 2G in Surkova et al. (Surkova et al., 2008)). This behavior also agrees with the previous result that the control of Hb sharpness and positioning by *hb* self-activation and Bcd cooperative binding, respectively, are separate processes that can be altered independently (Lopes et al., 2008). The results also agree with an n_H estimation that indicates that a coefficient greater than 10 is required for Hb sharpness (Houchmandzadeh et al., 2002).

Taken together, our results indicate that the apparent discrepancy between the various n_H can be accounted for by two time-dependent components. Early Bcd cooperative DNA binding sets up a later Hb self-regulation step, and together these are sufficient for establishing a sharp border of expression. Driver et al. noted that “One would not expect that such a mechanism immediately generates a sharp border … Subsequent regulatory interactions between *hb* and other zygotic genes might be involved in the establishment and maintenance of a border as sharp as that observed in later blastoderm stages” (Driever and Nusslein-Volhard, 1989). Lewis et al. used theoretical arguments to specifically propose that cooperative binding cannot account for sharp borders and that a self-activation mechanism is sufficient for sharp borders (Lewis et al., 1977). This last argument is also in agreement with the systems biology approach and proposal of Lopes et al. that *hb* self-activation via bistable kinetics is responsible for the sharp border of the Hb pattern (Lopes et al., 2008).

Crauk and Dostatni used lacZ constructs with three Bcd binding sites, and their results led them to propose that Bicoid determines sharp and precise *hb* expression (Crauk and Dostatni, 2005). However, three binding sites, even if they are strong, are not expected to provide full regulation of *hb* by Bcd as suggested by the authors. In addition, the experimental technique used, (non-fluorescent) *in situ* hybridization, can be affected by artificial saturation. Artificial saturation can occur depending on the reaction exposure time

and can increase the measurement of sharpness (see Fig. S3 in Lopes et al. (Lopes et al., 2008)). Other than *hb* itself, the two best candidates for having a role in Hb sharpening are *Kr* and *kni*. These candidates are best because of the relative position of their expression domains (*hb* domain is adjacent to *kni* and overlaps the *Kr* domain (Surkova et al., 2008; Tomancak et al., 2007)) and regulation of *hb* by *Kr* has previously been demonstrated (Jäckle et al., 1986; Treisman and Desplan, 1989). However, no effect on Hb sharpness was reported, even though *Kr;kni* double mutants showed disruptions in Hb pattern precision (Manu et al., 2009). In addition, there are discrepancies in the described effects of single mutations in *Kr* or *kni* on Hb positioning. Jäckle and collaborators reported an anterior shift of the Hb pattern in *Kr* mutant embryos (Jäckle et al., 1986), whereas Houchmandzadeh et al. reported no significant shift of the Hb pattern in *Kr* or *kni* single mutant embryos (Houchmandzadeh et al., 2002). However, the strong decrease in sharpness measured for the hb^{14F} allele (21.8% reduction, from 80.2° in WT to 62.8° in hb^{14F} (Lopes et al., 2008)) indicates that *Kr* or *kni* must have no effect on Hb sharpness because both of these genes are not affected in hb^{14F}. Finally, another explanation for the sharp border of the Hb pattern could be transcriptional synergy. It has been show that a greater than additive transcriptional response can be achieved by more than one activator acting simultaneously (Carey et al., 1990). However, experimental data that could indicate that this mechanism is responsible for the sharp Hb border are still needed. This mechanism could explain the enhanced n_H of pThb5 construct, however the effect of *hb* activation on this construct is dictated by the sharp border of the *hb* expression pattern. Because of this influence, it is difficult to distinguish between the contribution of transcriptional synergy and the sharp border of Hb pattern to the enhanced n_H of pThb5.

Acknowledgments

We thank John Reinitz for fruitful discussions on the model and for sharing lab facilities; David Holloway for discussions and exchanging of ideas; Steve Hanes and Ricardo Fabbri for manuscript revisions and comments; Ah-Ram Kim and the Bloomington Stock Center for providing lacZ probes and hb^{14F} flies, respectively; Carlos Alonso, Ah-Ram Kim, and Lisa Prazak for instructions on experiments; and Svetlana Surkova for helping with embryo temporal classification.

Acknowledgments

ROLE OF THE FUNDING SOURCE FJPL was supported by the Brazilian National Research Council (CNPq)/ Ministry of Science and Technology (MCT, Brazil), the Research Foundation of the State of Rio de Janeiro (FAPERJ, Brazil), grant 1-R01-GM072022 of the joint National Science Foundation (NSF)/National Institute of General Medical Sciences (NIGMS) BioMath program, and grant 2-ROI-RR07801 of the National Institutes of Health. PMB was supported by the CNPq/MCT, Brazil and the Research Foundation of the State of Rio de Janeiro (FAPERJ, Brazil). AVS was supported by grant 1-R01-GM072022 of the joint NSF/NIGMS BioMath program.

The study sponsors had no role in the study design or in the collection, analysis, or interpretation of data. The study sponsors were not involved in writing the report or in the decision to submit the paper for publication.

REFERENCES

Berleth T, et al. The role of localization of *bicoid* RNA in organizing the anterior pattern of the *Drosophila* embryo. Embo Journal. 1988; 7:1749–1756. [PubMed: 2901954]

Burz DS, Hanes SD. Isolation of mutations that disrupt cooperative DNA binding by the Drosophila Bicoid protein. Journal of Molecular Biology. 2001; 305:219–230. [PubMed: 11124901]

Burz DS, et al. Cooperative DNA-binding by Bicoid provides a mechanism for threshold-dependent gene activation in the Drosophila embryo. Embo Journal. 1998; 17:5998–6009. [PubMed: 9774343]

Carey M, et al. A mechanism for synergistic activation of a mammalian gene by GAL4 derivatives. Nature. 1990; 345:361–364. [PubMed: 2160609]

Crauk O, Dostatni N. Bicoid determines sharp and precise target gene expression on the Drosophila embryo. Current Biology. 2005; 15:1888–1898. [PubMed: 16271865]

de Lachapelle AM, Bergmann S. Precision and scaling in morphogen gradient read-out. Molecular Systems Biology. 2010; 6

Driever W, Nusslein-Volhard C. A gradient of *bicoid* protein in *Drosophila* embryos. Cell. 1988; 54:83–93. [PubMed: 3383244]

Driever W, Nusslein-Volhard C. The Bicoid protein Is a Positive regulator of *Hunchback* transcription in the early *Drosophila* embryo. Nature. 1989; 337:138–143. [PubMed: 2911348]

Driever W, et al. Determination of spatial domains of zygotic gene-expression in the *Drosophila* embryo by the affinity of binding-sites for the *Bicoid* morphogen. Nature. 1989; 340:363–367. [PubMed: 2502714]

Gregor T, et al. Probing the limits to positional information. Cell. 2007a; 130:153–164. [PubMed: 17632062]

Gregor T, et al. Stability and nuclear dynamics of the bicoid morphogen gradient. Cell. 2007b; 130:141–152. [PubMed: 17632061]

He F, et al. A Multiscale Investigation of Bicoid-Dependent Transcriptional Events in Drosophila Embryos. Plos One. 2011; 6

He F, et al. Shaping a Morphogen Gradient for Positional Precision. Biophysical Journal. 2010a; 99:697–707. [PubMed: 20682246]

He F, et al. Distance measurements via the morphogen gradient of Bicoid in Drosophila embryos. Bmc Developmental Biology. 2010b; 10

Hill AV. Proceedings of the Physiological Society. Journal of Physiology. 1910; 40

Holloway DM, et al. Gene Expression Noise in Spatial Patterning: *hunchback* Promoter Structure Affects Noise Amplitude and Distribution in *Drosophila* Segmentation. PLoS Comput Biol. 2011; 7:e1001069. [PubMed: 21304932]

Houchmandzadeh B, et al. Establishment of developmental precision and proportions in the early Drosophila embryo. Nature. 2002; 415:798–802. [PubMed: 11845210]

Hülskamp M, et al. Differential regulation of target genes by different alleles of the segmentation gene Hunchback in *Drosophila*. Genetics. 1994; 138:125–134. [PubMed: 8001780]

Jäckle H, et al. Cross-regulatory interactions among the gap genes of *Drosophila*. Nature. 1986; 324:668–670.

Jaeger J, et al. Dynamic control of positional information in the early Drosophila embryo. Nature. 2004; 430:368–371. [PubMed: 15254541]

Janssens H, et al. A high-throughput method for quantifying gene expression data from early Drosophila embryos. Development Genes and Evolution. 2005; 215:374–381. [PubMed: 15834586]

Lebrecht D, et al. Bicoid cooperative DNA binding is critical for embryonic patterning in Drosophila. Proceedings of the National Academy of Sciences of the United States of America. 2005; 102:13176–13181. [PubMed: 16150708]

Lehmann R, Nussleinvolhard C. Hunchback, a gene required for segmentation of an anterior and posterior region of the *Drosophila* embryo. Developmental Biology. 1987; 119:402–417. [PubMed: 3803711]

Lewis J, et al. Thresholds in Development. Journal of Theoretical Biology. 1977; 65:579–590. [PubMed: 859349]

Lopes FJP, et al. A kinetic mechanism for Drosophila Bicoid cooperative binding. Journal of Theoretical Biology. 2005; 235:185–198. [PubMed: 15862588]

Lopes FJP, et al. Spatial Bistability Generates hunchback Expression Sharpness in the Drosophila Embryo. PLoS computational Biology. 2008; 4

Lukowitz W, et al. Regulatory and coding regions of the segmentation gene *Hunchback* are functionally conserved between *Drosophila-virilis* and *Drosophila-melanogaster*. Mechanisms of Development. 1994; 45:105–115. [PubMed: 8199047]

Ma XG, et al. The Drosophila morphogenetic protein Bicoid binds DNA cooperatively. Development. 1996; 122:1195–1206. [PubMed: 8620846]

Manu, et al. Canalization of Gene Expression in the Drosophila Blastoderm by Gap Gene Cross Regulation. Plos Biology. 2009; 7:591–603.

Margolis JS, et al. Posterior stripe expression of Hunchback Is driven from 2 promoters by a common enhancer element. Development. 1995; 121:3067–3077. [PubMed: 7555732]

Merrill PT, et al. Requirements for autosomal gene activity during precellular stages of *Drosophila-melanogaster*. Development. 1988; 104:495–509. [PubMed: 3151484]

Moodley K, Murrell H. A colour-map plugin for the open source, Java based, image processing package, Image. J. Computers & Geosciences. 2004; 30:609–618.

Myasnikova E, et al. Estimation of errors introduced by confocal imaging into the data on segmentation gene expression in Drosophila. Bioinformatics. 2009; 25:346–352. [PubMed: 19052059]

Nusslein-Volhard C, et al. Determination of anteroposterior polarity in *Drosophila*. Science. 1987; 238:1675–1681. [PubMed: 3686007]

Papatsenko D, Levine M. The Drosophila Gap Gene Network Is Composed of Two Parallel Toggle Switches. PLoS ONE. 2011; 6:e21145. [PubMed: 21747931]

Papatsenko D, Levine MS. Dual regulation by the Hunchback gradient in the Drosophila embryo. Proceedings of the National Academy of Sciences of the United States of America. 2008; 105:2901–2906. [PubMed: 18287046]

Poustelnikova E, et al. A database for management of gene expression data in situ. Bioinformatics. 2004; 20:2212–2221. [PubMed: 15059825]

Schroder C, et al. Differential regulation of the 2 transcripts from the *Drosophila* gap segmentation gene *Hunchback*. Embo Journal. 1988; 7:2881–2887. [PubMed: 2846287]

Simpson-Brose M, et al. Synergy between the Hunchback and Bicoid morphogens is required for anterior patterning in *Drosophila*. Cell. 1994; 78:855–865. [PubMed: 8087852]

Spirov AV, et al. HOX Pro DB: the functional genomics of hox ensembles. Nucleic Acids Research. 2002; 30:2.

Spirov AV, et al. HOX Pro: a specialized database for clusters and networks of homeobox genes. Nucleic Acids Research. 2000; 28:3.

Struhl G, et al. The gradient morphogen Bicoid is a concentration-dependent transcriptional activator. Cell. 1989; 57:1259–1273. [PubMed: 2567637]

Stryer, L. Biochemistry. Freeman; New York: 1995.

Surkova S, et al. Characterization of the Drosophila segment determination morphome. Developmental Biology. 2008; 313:844–862. [PubMed: 18067886]

Tautz D, et al. Finger protein of novel structure encoded by Hunchback, a 2nd member of the gap class of *Drosophila* segmentation genes. Nature. 1987; 327:383–389.

Tomancak P, et al. Global analysis of patterns of gene expression during Drosophila embryogenesis. Genome Biology. 2007; 8

Treisman J, Desplan C. The products of the *Drosophila* gap genes *Hunchback* and krüppel bind to the *Hunchback* promoters. Nature. 1989; 341:335–337. [PubMed: 2797150]

Highlights

- Bcd cooperative binding to the native *hunchback* promoter exhibits a Hill coefficient of approximately 3.0.
- A Hill coefficient of approximately 10.0 is necessary for sharp, mature Hunchback patterning.
- Bicoid cooperative binding cannot account for sharpness in the mature Hunchback pattern.
- Self-activation of *hunchback* is necessary to produce the sharp border of the mature Hunchback pattern.

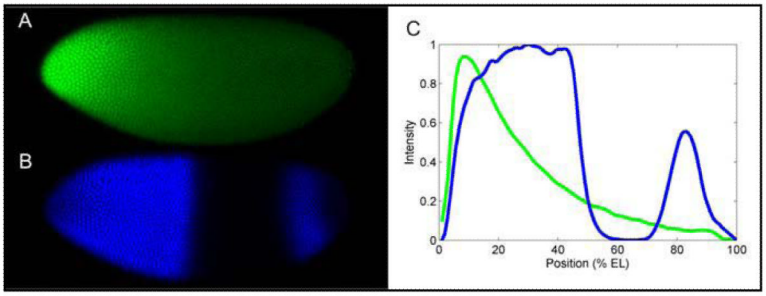

Fig. 1. Hb and Bcd protein profiles (Lopes et al., 2008)

An embryo at mid-nuclear cleavage cycle 14A immunostained for Bcd (**A**) and Hb (**B**). (**C**) Fluorescence intensities for A and B are shown in green and blue, respectively, as a function of position along the AP axis. The diffusion of Bcd protein, translated from its mRNA localized at the anterior end of the egg, forms an exponential concentration gradient. In A and B, the anterior pole is on left and the dorsal side is on top.

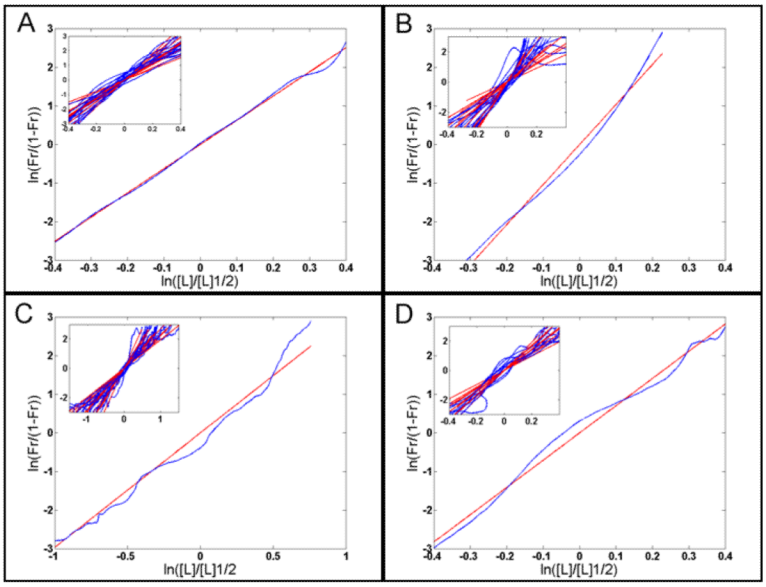

Fig. 2. Estimating the required Hill coefficient to pattern Hb profiles in embryos of different stages or backgrounds (Lopes et al., 2008)

The Hill coefficient is given by the inclination of the straight line (see equation (2) in Material and Methods). **(A)**: Plot from a WT embryo at early cycle 14A exhibiting an n_H of 6.3 that is similar to the mean n_H (6.3, *s.d.* 1.4) measured from 15 embryos at this stage (inset). **(B)**: The same plot as in (A) but from a WT embryo at late cycle 14A with an n_H of approximately 11.6 that is similar to the mean n_H (10.8, *s.d.* 4.0) measured from 15 embryos at this stage (inset). **(C)**: Same plot as in (A) but from an hb^{14F} embryo at cycle 14A with an n_H of approximately 3.0. Inset: 15 embryos at this stage with the mean n_H (3.0, *s.d.* 1.0). **(D)**: The same plot as above from an embryo expressing the pThb5 lacZ artificial construct at cycle 14A and exhibiting an n_H of 7.0. Inset: 9 embryos with mean n_H (7.0, *s.d.* 1.5). We assumed early and late cycle 14A embryos corresponded to stages T1-T4 and T5-T6, respectively, according to previous classification (Surkova et al., 2008).

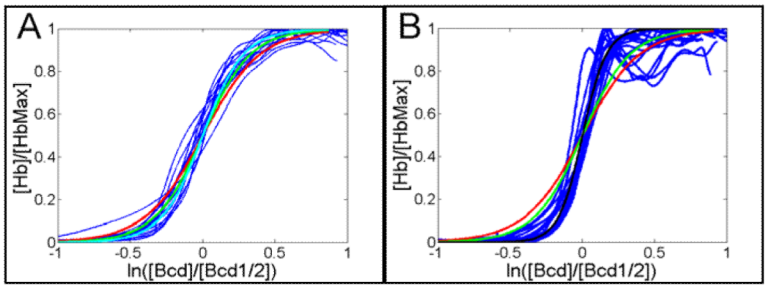

Fig. 3. Estimating the required Hill coefficient to account for Hb sharpness using an alternative plot

(A) The same data from the 15 WT early embryos used for Fig. 2A but plotted similarly to Fig. 4A by Gregor et al. (Gregor et al., 2007a). **(B)** The same 15 WT late embryos as in Fig. 2B but plotted as in A. In these graphics, the red, green, cyan and black lines show the plots for an n_H of 5, 6, 7 and 10, respectively. It is easy to see that in (A), the n_H choice of 6 fits the data better, while in (B), the best choice is 12. This method (see equation (1) in Material and Methods) does not allow a precise determination of n_H because visual inspection is used. The straight-line fitting, used for Figs. 2 and 4, is more precise and accurate.

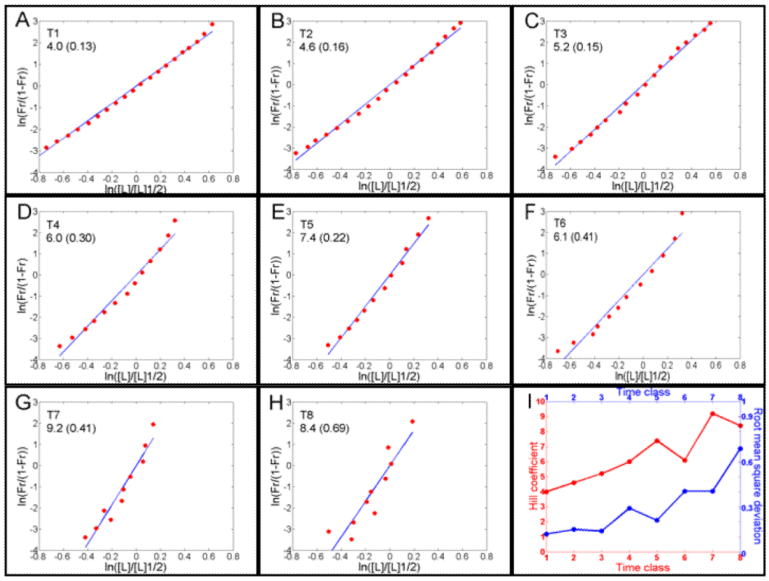

Fig. 4. Required Hill coefficients for each temporal class in cycle 14A necessary to account for Hb sharpness as determined from averaged data

Poustelnikova et al., 2004; Surkova et al., 2008)**(A) – (H):** Plots for time classes T1-T8, which last for approximately 6 minutes each. The Hill coefficients, shown in the insets followed by the *r.m.s.d.*, were determined by the straight-line inclination of these plots. **(I)**: Evolution of the Hill coefficient (red line) from A to H and *r.m.s.d.* (blue line) as a function of time classes. The increase in *r.m.s.d.* indicates a reduction in how suitable the Hill approach is for describing this system. The increase in n_H indicates that Bcd cooperative binding cannot account for the sharpness of the Hb pattern after T4. To generate these plots, we used the equation (2) in Material and Methods.

Table 1

Estimating the required Hill coefficient to account for Hb sharpness in embryos at different stages of cycle 14 or with different backgrounds.

	Background	Mean n_H (*s.d.*/mean *r.m.s.d.*)	Number of embryos	Age (minutes)
	*hb*14F	3.0 (1.0/0.25)	15	32-39
	early WT	6.3 (1.4/0.20)	15	4-23
	late WT	10.8 (4.0/0.35)	15	26-53
lacZ		7.0 (1.5/0.36)	9	20-37